Herschel/SPIRE FTS View of M82

Probing the molecular ISM in M82 starburst

Pasquale Panuzzo (CEA Saclay Irfu/SAp) and SAG2:

N. Rangwala, A. Rykala, K. G. Isaak, J. Glenn, C. D. Wilson, L. Spinoglio, M. Bradford, R. Auld, M. Baes, M. J. Barlow,G. J. Bendo, J. J. Bock, A. Boselli, V. Buat, N. Castro-Rodríguez, P. Chanial, S. Charlot, L. Ciesla, D. L. Clements, A. Cooray, D. Cormier, L. Cortese, J. I. Davies, E. Dwek, S. A. Eales, D. Elbaz, T. Fulton, M. Galametz, F. Galliano, W. K. Gear, H. L. Gomez, M. Griffin, S. Hony, L. R. Levenson, N. Lu, S. Madden, B. O'Halloran, K. Okumura, S. Oliver, M. J. Page, A. Papageorgiou, T. J. Parkin, I. Pérez-Fournon, M. Pohlen, E. T. Polehampton, E. E. Rigby, H. Roussel, N. Sacchi, M. Sauvage, B. Schulz, M. R. P. Schirm, M. W. L. Smith, J. A. Stevens, S. Srinivasan, M. Symeonidis, B. Swinyard, M. Trichas, M. Vaccari, L. Vigroux, H. Wozniak, G. S. Wright, W. W. Zeilinger

M82 SPIRE FTS observations

- M82 is the nearest (3.9Mpc) starburst (~10Msun/yr)
  - Brightest IRAS extragalactic source (1390Jy at 100μm)
  - Widely used in cosmology as starburst prototype
- Target of the *Very Nearby Galaxies Survey* (SAG2)
- M82 was observed as Performance Verification target
  - High resolution (FWHM=0.048 cm^{-1} R~1000)
  - 1332 seconds (10 repetitions)
  - Point source mode (single staring pointing)

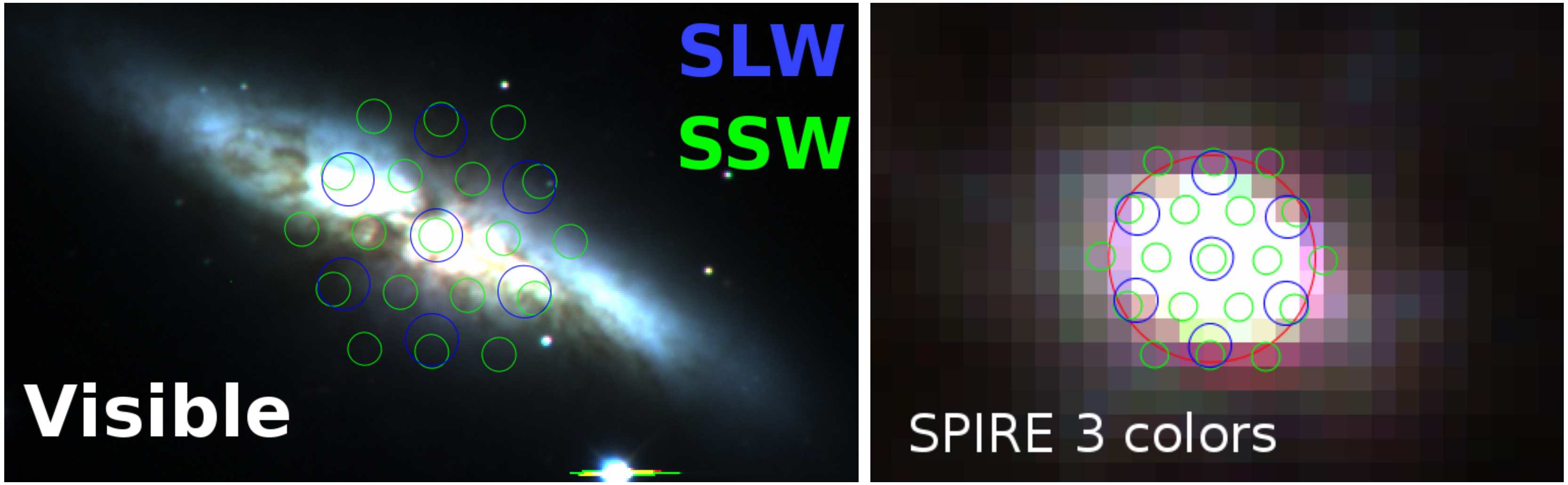

Data analysis

- Processed with customized version of HIPE3 pipeline
  - We used only data of central detectors
  - M82 was detected also on first ring detectors
- Beam size of the FTS bolometers varies with wavelength
- Spatial extent of the M82 central starburst is comparable to the beam size
  - M82 is not a point source nor an extended flat source for FTS bolometers

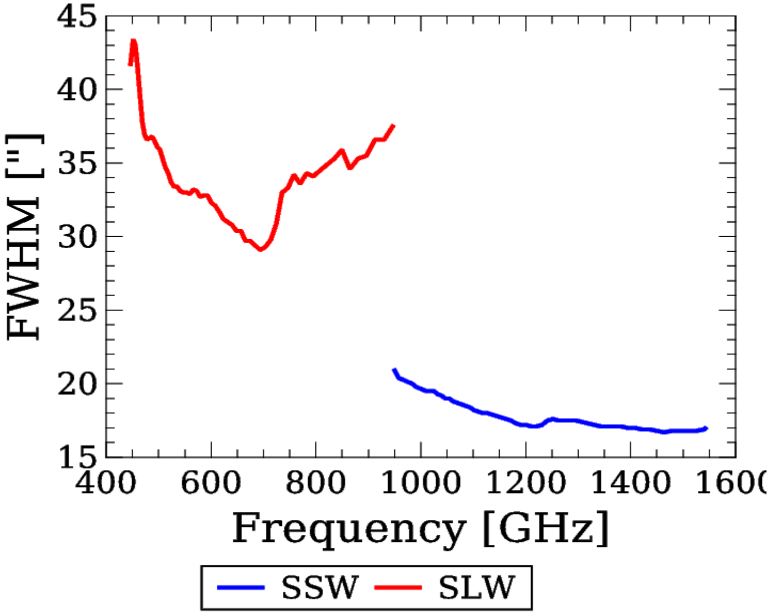

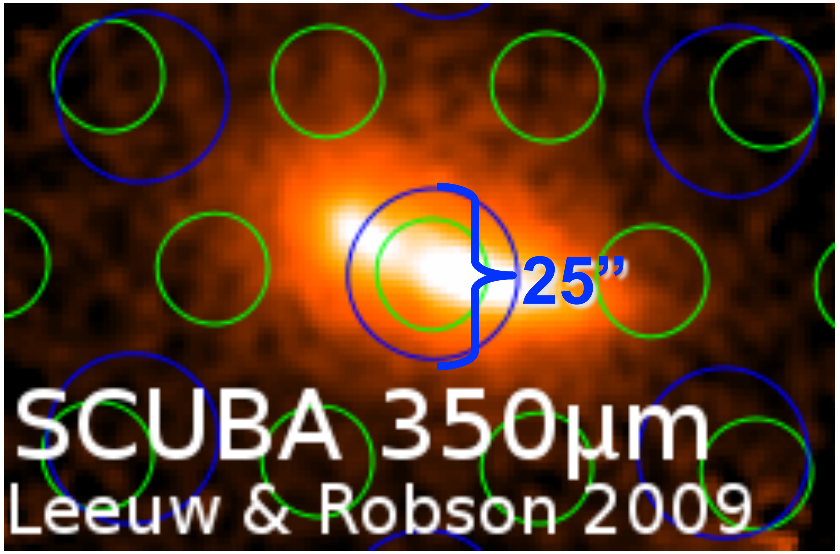

Source-beam coupling correction

- To compare the SED with models, we need to scale the spectrum to a single beam size with a source-beam coupling factor η(λ)
  - Largest beam size is 43.4”
- We assume Gaussian beams [$b(\underline{x},\mathrm{FWHM}(\lambda))$] and same light distribution [$f(\underline{x})$] at all wavelengths [λ]
  - CO line maps are not so different from continuum emission distribution
- The source-beam coupling factor is given by:

$$\eta(\lambda) = [\int f(\underline{x})b(\underline{x},\mathrm{FWHM}(\lambda))d\Omega] / [\int f(\underline{x})b(\underline{x},43.4'')d\Omega]$$

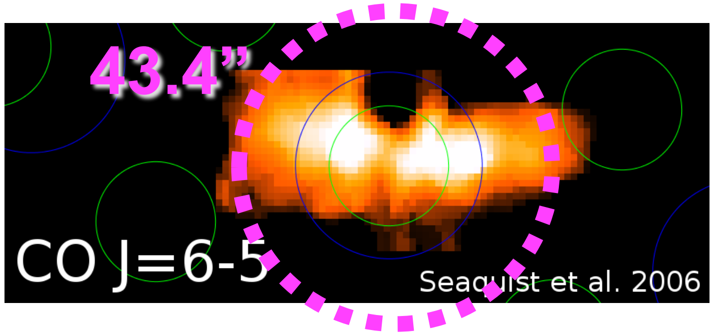

Seaquist et al. 2006

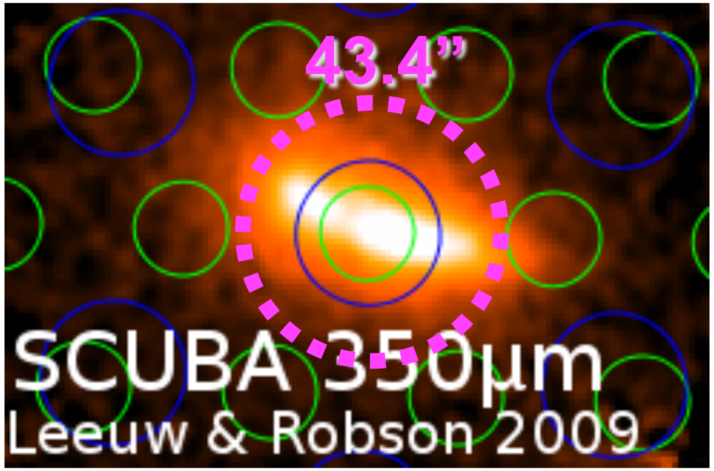

Leeuw & Robson 2009

Source-beam coupling correction (2)

- The value of $\int f(\underline{x})b(\underline{x},\mathrm{FWHM}(\lambda))\,d\Omega$ was determined convolving M82 250μm maps with a gaussian beam $b'(\underline{x},\sqrt{(\mathrm{FWHM}^2-18.1''^2)})$
- Extended-source flux calibration (based on telescope modelling) is less noisy than point-source flux calibration but gives fluxes 2x fainter than photometry
  - Known problem, under analysis
- We had to multiply by another scaling factor to match photometry in the same beam

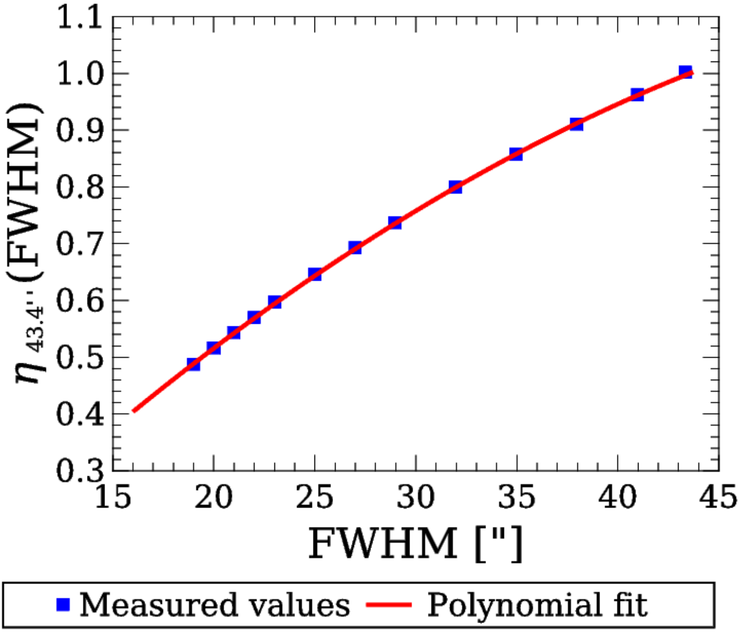

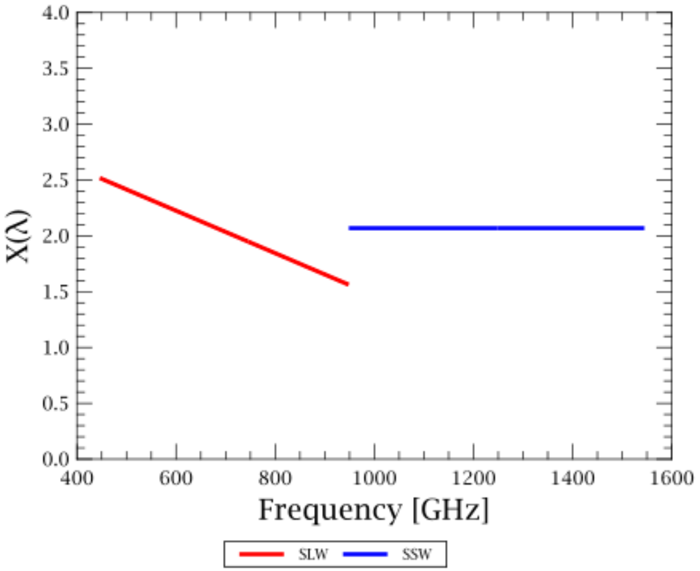

M82 reconstructed apodized spectrum

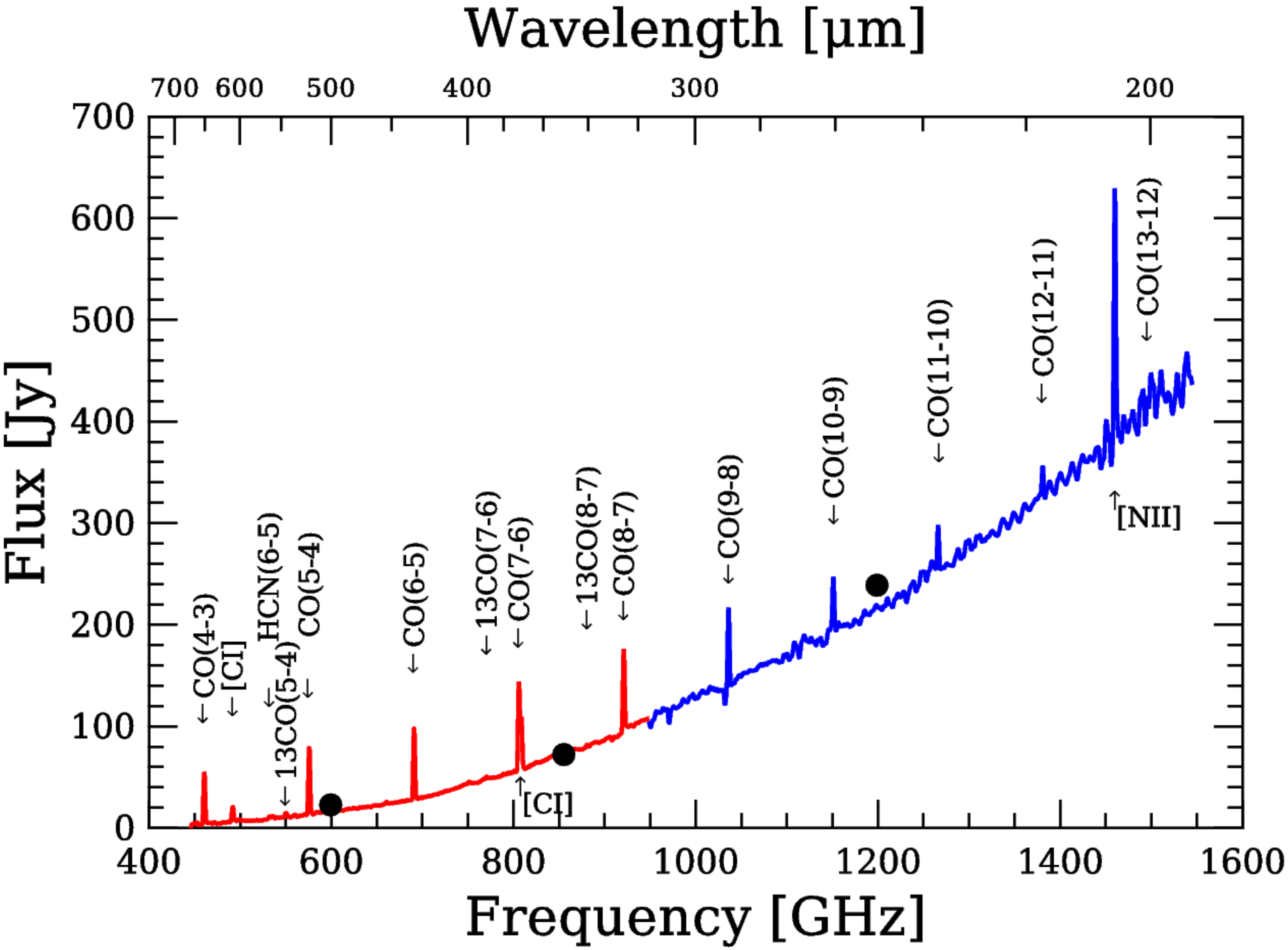

Line extraction

- Emission line extraction from un-apodized spectrum with SLIDE tool
  - Remove continuum (graybody + polynomial)
  - Fit strongest line with sinc-convolved gaussian
  - Remove the fitted line and iterate on the residual
- Detected lines:
  - ^{12}CO J=4-3 up to J=13-12
  - 3 ^{13}CO lines (+1)
  - 1 HCN line
  - 2 [CI] and [NII] lines
- Additional error ~30% (1σ) from corrections / calibration

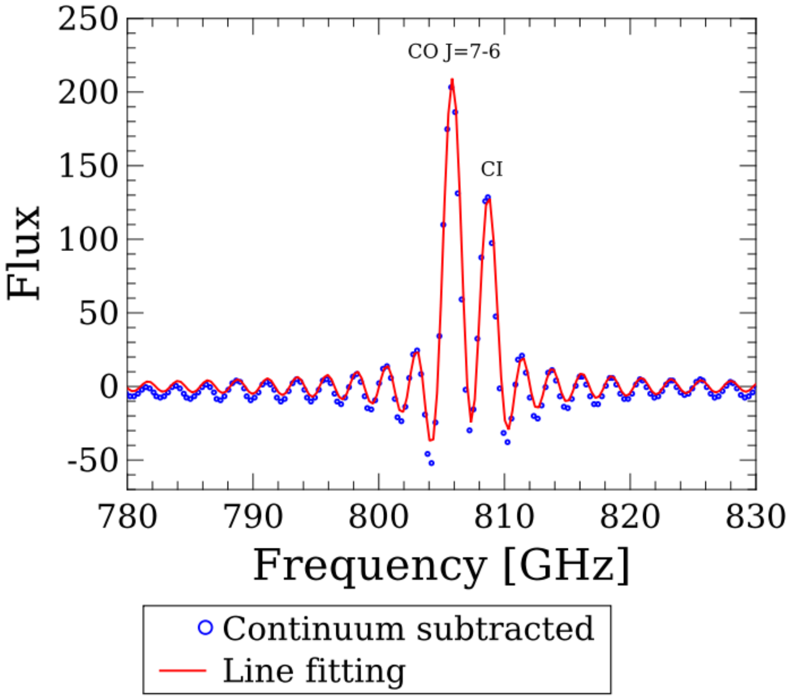

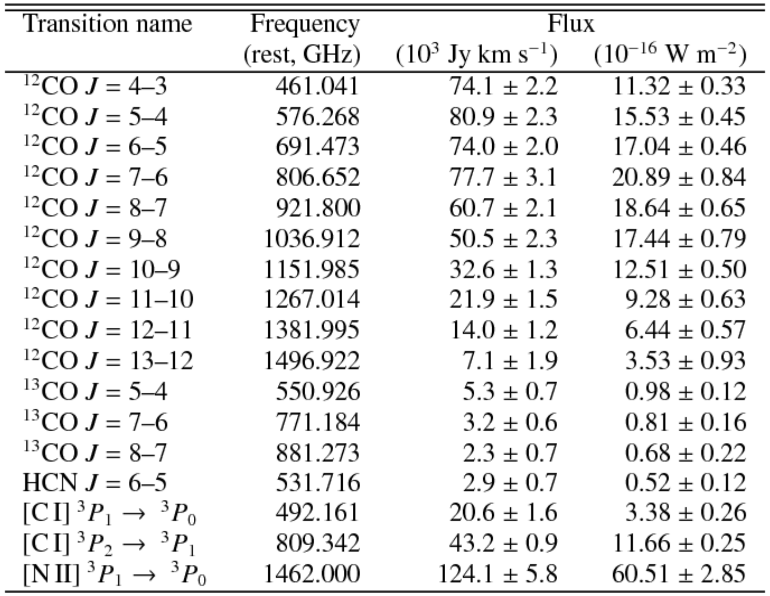

Transition name	Frequency	Flux	
	(rest, GHz)	(10^3 Jy km s^{-1})	(10^{-16} W m^{-2})
^{12}CO $J = 4–3$	461.041	74.1 ± 2.2	11.32 ± 0.33
^{12}CO $J = 5–4$	576.268	80.9 ± 2.3	15.53 ± 0.45
^{12}CO $J = 6–5$	691.473	74.0 ± 2.0	17.04 ± 0.46
^{12}CO $J = 7–6$	806.652	77.7 ± 3.1	20.89 ± 0.84
^{12}CO $J = 8–7$	921.800	60.7 ± 2.1	18.64 ± 0.65
^{12}CO $J = 9–8$	1036.912	50.5 ± 2.3	17.44 ± 0.79
^{12}CO $J = 10–9$	1151.985	32.6 ± 1.3	12.51 ± 0.50
^{12}CO $J = 11–10$	1267.014	21.9 ± 1.5	9.28 ± 0.63
^{12}CO $J = 12–11$	1381.995	14.0 ± 1.2	6.44 ± 0.57
^{12}CO $J = 13–12$	1496.922	7.1 ± 1.9	3.53 ± 0.93
^{13}CO $J = 5–4$	550.926	5.3 ± 0.7	0.98 ± 0.12
^{13}CO $J = 7–6$	771.184	3.2 ± 0.6	0.81 ± 0.16
^{13}CO $J = 8–7$	881.273	2.3 ± 0.7	0.68 ± 0.22
HCN $J = 6–5$	531.716	2.9 ± 0.7	0.52 ± 0.12
[C I] $^3P_1 \rightarrow {}^3P_0$	492.161	20.6 ± 1.6	3.38 ± 0.26
[C I] $^3P_2 \rightarrow {}^3P_1$	809.342	43.2 ± 0.9	11.66 ± 0.25
[N II] $^3P_1 \rightarrow {}^3P_0$	1462.000	124.1 ± 5.8	60.51 ± 2.85

M82 ^{12}CO SLED

- The Spectral Line Emission Distribution (SLED) of ^{12}CO peaks at J=7-6
- Low J lines taken from Ward et al (2003) in a similar area
- Only with Herschel we can determine the peak of the SLED

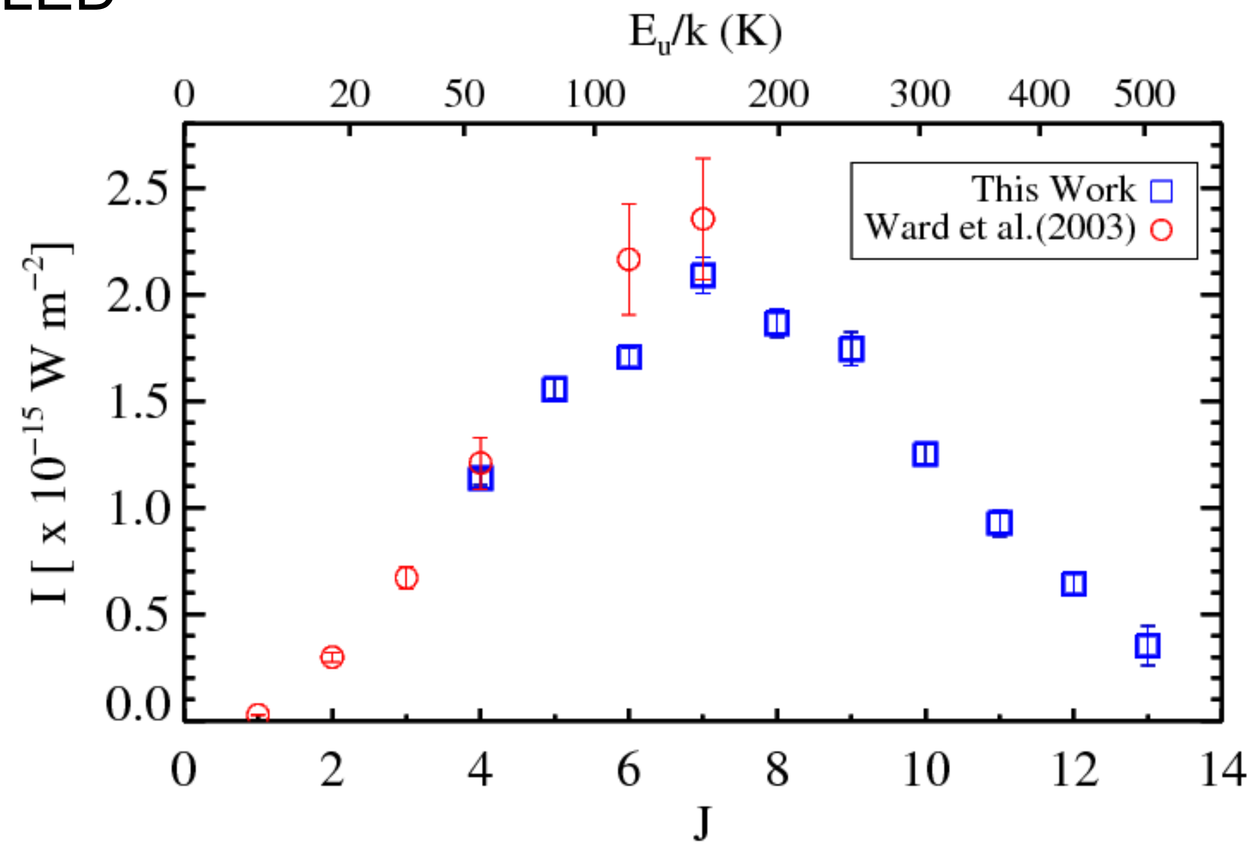

RADEX modelling

- We used RADEX (van det Tak et al 2007) non-LTE code to compute ^{12}CO and ^{13}CO lines for a large parameter grid
  - T_{kin}: 20-1000K; n_{H2}: 100-10^6cm^{-3}; N(^{12}CO): 10^{15}-10^{18}cm^{-2}; N (^{13}CO): 10^{13}-10^{17}cm^{-2}
- We computed the likelihood of each model
  - A single component was assumed
  - Had to add 20% uncertainty for lines in SLW and 10% in lines in SSW range

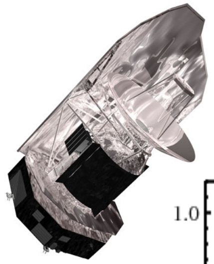

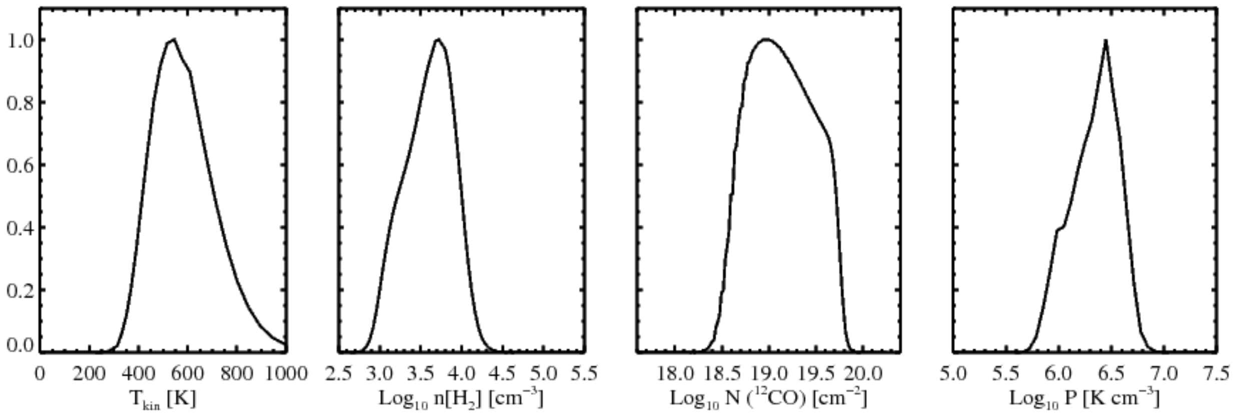

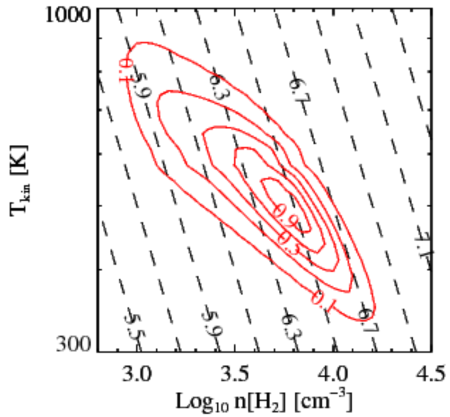

Modelled ^{12}CO SLED

- SPIRE-detected CO lines well reproduced by a warm (T_{kin} = 545 K) molecular gas component with mass 1.2 x 10^7Msun
- Same temperature of H2 S(1) – S(2) MIR lines

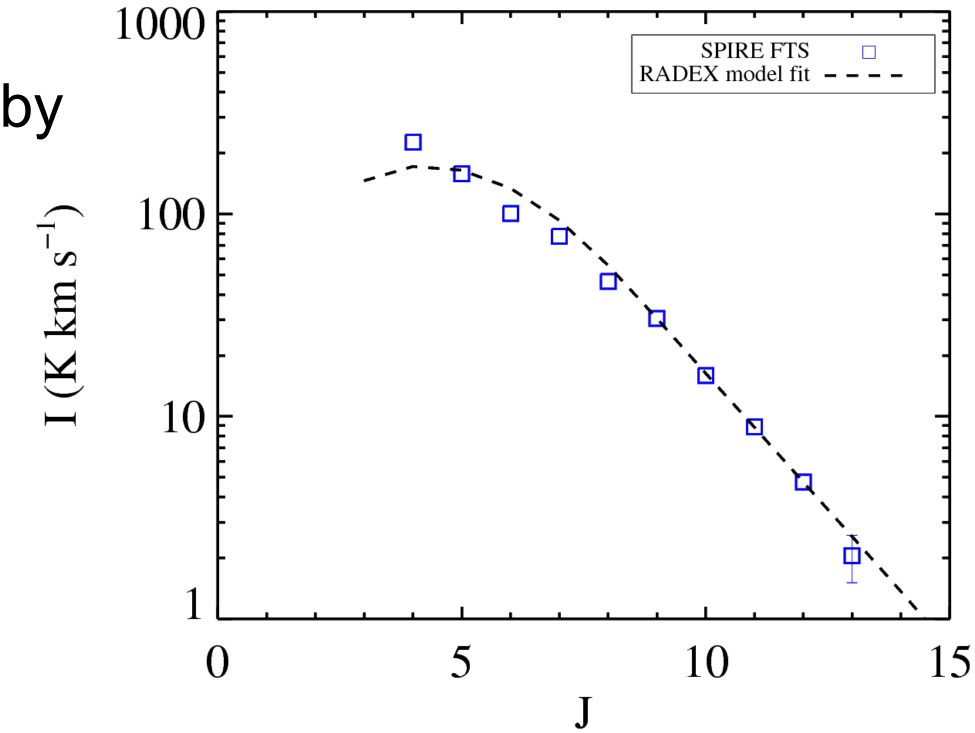

Quantity	Most Probable Value	range[†]
$T_{\rm kin}$ (K)	545	350 – 825
$\mathrm{Log}_{10}\, n(\mathrm{H_2})$ (cm^{-3})	3.7	3.0 – 4.1
$\mathrm{Log}_{10} N(^{12}\mathrm{CO})$ (cm^{-2})	19.0	18.5 – 19.8
$\mathrm{Log}_{10}\, \Phi_A N(^{12}\mathrm{CO})^{\ddagger}$ (cm^{-2})	17.4	17.2 – 17.9
$N(^{12}\mathrm{CO})/N(^{13}\mathrm{CO})$	20	15 – 37
$\mathrm{Log}_{10} P$ (K cm^{-3})	6.4	5.8 – 6.7
$M_{\rm gas}$ ($\times 10^7$ M$_\odot$)	1.2	0.7 – 3.6

SPIRE + ground-based SLED

- Low J lines dominated by cold gas, as determined by various ground-based works
- The sum of 2 components (cold at ~25K, warm at ~550K) reproduce well the entire SLED (SPIRE + ground data)
- Mass of cold gas is ~3 times the mass of warm gas
  - Warm and cold components have similar pressure

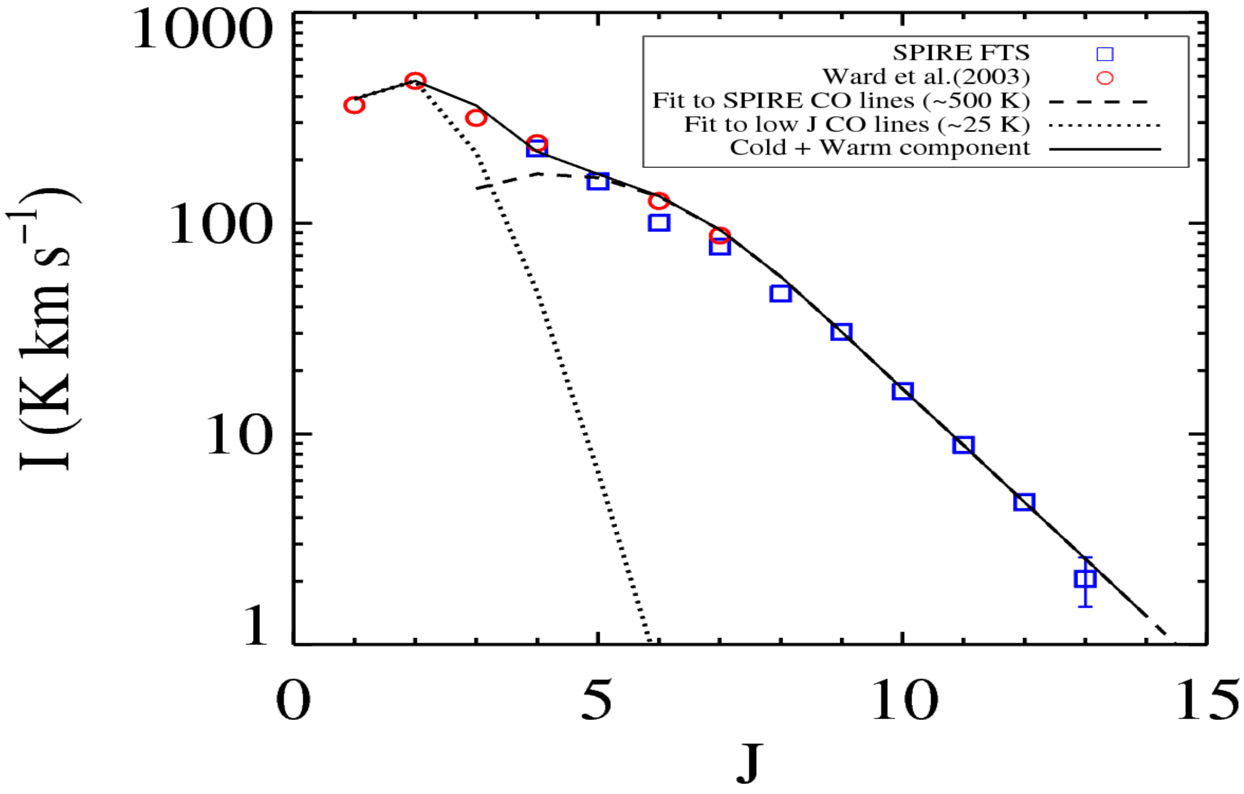

Heating and cooling mechanisms

- At ~500K MIR H_2 rotational lines are the dominant coolant
  - CO luminosity ~ 5 x 10^6 Lsun
  - H_2 luminosity ~ 3 x 10^7 Lsun (Beirão et al. 2008)
  - [CI] lines (491+809 GHz) ~ 5.4 x 10^5 Lsun
- We considered several heating mechanisms as responsible for the warm molecular gas:
  - UV powered PDRs: observed CO lines too luminous compared with PDR models; would need too high density
  - X-ray powered XDRs: X-ray luminosity too low, and SLED decreases at high J (contrary to XDR-dominate Mkr231 in Loenen talk)
  - Cosmic ray: would need > 10 times CR rate of MW
  - Dissipation of turbulence (Falgarone & Puget 1995, Pan & Padoan 2009): from velocity gradient from RADEX (~35km/s/pc), turbulence can match the observed cooling

Conclusions

- We have presented the Herschel-SPIRE spectroscopic observations of the starburst galaxy M82.
- We derived a source-beam coupling correction to scale the observed spectrum to a single beam
- Prominent CO ladder along with [C I] and [N II] lines.
- Modelling of CO lines clearly indicates the presence of a warm gas component at ~550K in addition to the cold (~25K) component found by ground-based studies.
- The temperature and mass of warm gas are in agreement with the H_2 rotational lines observations from Spitzer and ISO.
- H_2 is the dominant coolant instead of CO
- Turbulence generated by stellar winds and supernovae may be the dominant heating mechanism.